Earlier Snowmelt May Lead to Late Season Declines in Plant Productivity and Carbon Sequestration in Arctic Tundra Ecosystems

Donatella Zona (dzona@sdsu.edu)
San Diego State University
Peter Lafleur
Trent University
Koen Hufkens
UMR 1391 ISPA, INRA, 71 avenue Edouard Bourlaux, 33140, Villenave D'Ornon, France
Barbara Bailey
San Diego State University
Beniamino Gioli
National Research Council
George Burba
Licor Environmental
Jordan Goodrich
University of Waikato
Anna Liljedahl
Woodwell Climate Research Center, Falmouth, MA 02540, USA
Eugenie Euskirchen
University of Alaska Fairbanks
Jennifer Watts
Woodwell Climate Research Center, Falmouth, MA 02540, USA
Mary Farina
Woodwell Climate Research Center, Falmouth, MA 02540, USA
John Kimball
University of Montana
Martin Heimann
Max Planck Institute for Biogeochemistry
Mathias Goeckede
Max Planck Institute for Biogeochemistry
Martijn Pallandt
Max Planck Institute for Biogeochemistry
Torben Christensen

Aarhus University
Mikhail Mastepanov
Aarhus University
Efren Lopez-Blanco
Aarhus University
Marcin Jackowicz-Korczynski
Aarhus University
Albertus J. Dolman
VU Amsterdam
Luca Belelli Marchesini
Fondazione Edmund Mach
Roisin Commane
Columbia University
Steve Wofsy
Harvard University
Charles Miller
Jet Propulsion Lab
David Lipson
San Diego State University
Josh Hashemi
San Diego State University
Kyle Arndt
University of New Hampshire
Lars Kutzbach
Universität Hamburg
David Holl
Universität Hamburg
Julia Boike
Humboldt-Universität zu Berlin
Christian Wille
Helmholtz Centre Potsdam - GFZ German Research Centre for Geosciences
Torsten Sachs
Helmholtz Centre Potsdam - GFZ German Research Centre for Geosciences
Aram Kalhori
Helmholtz Centre Potsdam - GFZ German Research Centre for Geosciences
Xia Song
San Diego State University
Xiaofeng Xu
San Diego State University

Elyn Humphreys
Carleton University
Charles Koven
Lawrence Berkeley National Laboratory
Oliver Sonnentag
University of Montreal
Gesa Meyer
University of Montreal
Gabriel Gosselin
University of Montreal
Philip Marsh
University of Waterloo
Walter Oechel
San Diego State University

Research Article

Keywords: permafrost, carbon loss, climate change, wetlands, snowmelt, plant productivity, senescence

Posted Date: October 18th, 2021

DOI: https://doi.org/10.21203/rs.3.rs-959226/v1

Version of Record: A version of this preprint was published at Scientific Reports on March 21st, 2022. See the published version at https://doi.org/10.1038/s41598-022-07561-1.

Earlier snowmelt may lead to late season declines in plant productivity and carbon sequestration in Arctic tundra ecosystems

Donatella Zona[1,2,*], Peter M. Lafleur[3], Koen Hufkens[4,5], Barbara Bailey[1], Beniamino Gioli[6], George Burba[7,8], Jordan P. Goodrich[9], Anna K. Liljedahl[10,11], Eugénie S. Euskirchen[12], Jennifer D. Watts[11,13], Mary Farina[11], John S. Kimball[13], Martin Heimann[14,15], Mathias Göckede[14], Martijn Pallandt[14], Torben R. Christensen[16,17], Mikhail Mastepanov[16,17], Efrén López-Blanco[16,18], Marcin Jackowicz-Korczynski[16,19], Albertus J. Dolman[20], Luca Belelli Marchesini[21,22], Roisin Commane[23], Steven C. Wofsy[24], Charles E. Miller[25], David A. Lipson[1], Josh Hashemi[1], Kyle A. Arndt[26], Lars Kutzbach[27], David Holl[27], Julia Boike[28,29], Christian Wille[30], Torsten Sachs[30], Aram Kalhori[30], Xia Song[1] Xiaofeng Xu[1], Elyn R. Humphreys[31], Charles D. Koven[32], Oliver Sonnentag[33], Gesa Meyer[33], Gabriel H. Gosselin[33], Philip Marsh[34], Walter C. Oechel[1,35]

[1]Department Biology, San Diego State University, San Diego, CA 92182, USA
[2]Department of Animal and Plant Sciences, University of Sheffield, Western Bank, Sheffield, S10 2TN, United Kingdom
[3]School of the Environment, Trent University, Peterborough, ON K9L 0G2, Canada
[4]UMR 1391 ISPA, INRA, 71 avenue Edouard Bourlaux, 33140, Villenave D'Ornon, France
[5]Department of Applied Ecology and Environmental Biology, Ghent University, 653, 9000, Ghent, Belgium
[6]IBE, National Research Council (CNR), Institute of BioEconomy, via Giovanni Caproni 8, Firenze, 50145, Italy
[7]LI-COR Biosciences, 4421 Superior St., Lincoln, NE, 68504, USA
[8]The Robert B. Daugherty Water for Food Global Institute and School of Natural Resources, University of Nebraska, Lincoln, NE, 68583
[9]Department of Earth Sciences, University of Waikato, Hillcrest, Hamilton 3216, New Zealand
[10]Water and Environmental Research Center, University of Alaska Fairbanks, Fairbanks, AK 99775-7340, USA
[11]Woodwell Climate Research Center, Falmouth, MA 02540, USA
[12]Institute of Arctic Biology, University of Alaska Fairbanks, Fairbanks, AK, 99775, USA

[13]W.A. Franke College of Forestry & Conservation, The University of Montana, Missoula, MT, 59812, USA
[14]Max Planck Institute for Biogeochemistry, 07745 Jena, Germany.
[15]University of Helsinki, Faculty of Science, Institute for Atmospheric and Earth System Research (INAR) / Physics, P.O. Box 64 FI-00014 University of Helsinki, Finland, Gustaf Hällströmin katu 2b, 00560 Helsinki
[16]Department of Bioscience, Arctic Research Centre, Aarhus University, Frederiksborgvej 399, 4000 Roskilde, Denmark
[17]Oulanka Research Station, Oulu University, Kuusamo, Finland
[18]Greenland Institute of Natural Resources, Department of Environment and Minerals, 3900 Nuuk, Greenland
[19]Department of Physical Geography and Ecosystem Science, 22362 Lund University, Lund, Sweden
[20]Department of Earth Sciences, Vrije Universiteit Amsterdam, 1081HV Amsterdam, The Netherlands
[21]Dept. of Sustainable Agro-Ecosystems and Bioresources, Research and Innovation Centre, Fondazione Edmund Mach, via E. Mach 1, 38010 San Michele all'Adige (TN) Italy
[22]Agrarian-Technological Institute, RUDN University, 117198 Moscow, Russia
[23]Dept of Earth and Environmental Sciences, Columbia University, Lamont-Doherty Earth Observatory, Palisades, NY 10964
[24]School of Engineering and Applied Sciences, Harvard University, 20 Oxford St., Cambridge, MA 02138, USA
[25]Jet Propulsion Laboratory, California Institute of Technology, 4800 Oak Grove Drive, Pasadena, CA 91109-8099, USA
[26]Earth Systems Research Center, Institute for the Study of Earth, Oceans, and Space, 8 College Rd, University of New Hampshire, Durham, NH, 03824, United States
[27]Institute of Soil Science, Center for Earth System Research and Sustainability (CEN), Universität Hamburg, 20146 Hamburg, Germany
[28]Geography Department, Humboldt-Universität zu Berlin, 10099 Berlin, Germany
[29]Alfred Wegener Institute Helmholtz Centre for Polar and Marine Research, 14473, Potsdam, Germany
[30]GFZ German Research Centre for Geosciences, 14473 Potsdam, Germany
[31]Department of Geography & Environmental Studies, Carleton University, Ottawa, ON K1S 5B6 Canada
[32]Climate and Ecosystem Sciences Division, Lawrence Berkeley National Laboratory (LBNL), Berkeley, CA 94720, USA
[33]Département de Géographie, Université de Montréal, 1375 Avenue Thérèse-Lavoie-Roux, Montréal, QC H2V 0B3, Canada
[34]Wilfrid Laurier University, Department of Geography and Environmental Studies, 75 University Ave W., Waterloo, ON, Canada, N2S 3C5
[35]Department of Geography, College of Life and Environmental Sciences, University of Exeter, Exeter, EX4 4RJ, UK

*corresponding author email: dzona@sdsu.edu; D.zona@sheffield.ac.uk

Abstract

Arctic warming is affecting snow cover and soil hydrology, with consequences for carbon sequestration in tundra ecosystems. The scarcity of observations in the Arctic has limited our understanding of the impact of covarying environmental drivers on the carbon balance of tundra ecosystems. In this study, we address some of these uncertainties through a novel record of 119 site-years of summer data from eddy covariance towers representing dominant tundra vegetation types located on continuous permafrost in the Arctic.

Here we found that earlier snowmelt was associated with more net CO_2 sequestration and higher gross primary productivity (GPP) only in June and July, but with lower net carbon sequestration and lower GPP in August. Although higher evapotranspiration (ET) can result in soil drying with the progression of the summer, we did not find significantly lower soil moisture with earlier snowmelt, nor evidence for a water stress that affected GPP in the peak and late growing season. Our results suggest that climate change and the associated increased length in the growing season might not benefit these northern tundra ecosystems if they are not able to continue sequestering CO_2 later in the season.

Keywords: permafrost, carbon loss, climate change, wetlands, snowmelt, plant productivity, senescence

Climate change is affecting arctic ecosystems through temperature increase (Overland et al., 2019), hydrological changes (Liljedahl et al., 2016), earlier snowmelt (Mudryk et al., 2017; 2019) and the associated increase in growing season length (Piao et al., 2020). Annual arctic air temperature has been increasing at more than double the magnitude of the global mean air temperature increase (Overland et al., 2019), and terrestrial snow cover in June has decreased by 15.2% per decade from 1981–2019 (Mudryk et al., 2019). Warming is a main driver of the earlier start of the growing season and of the greening of the Arctic (Lucht et al., 2002; Berner et al., 2020; Myers-Smith et al., 2020). Arctic greening is associated with enhanced vegetation height, biomass, cover and abundance (Forbes et al., 2010). However, the complexity of arctic systems reveals an intricate patchwork of landscape greening and browning (Lara et al., 2018; Miles et al., 2016; Myers-Smith et al., 2020), with browning linked to a variety of stresses to vegetation (Myers-Smith et al., 2020) including water stress (Gonsamo et al., 2019; Gamm et al., 2018). The interconnected changes in temperature, soil moisture, snowmelt timing, etc. can have important effects on the carbon sequestered by arctic ecosystems (Bruhwiler et al., 2021). The reservoir of carbon in arctic soil and vegetation depends on the interaction of two main processes: 1) changes in net CO_2 uptake by vegetation; and 2) increased net loss of CO_2 (from vegetation and soil respiration) to the atmosphere via enhanced respiration. Therefore, defining the response of both plant productivity and ecosystem respiration to environmental changes is needed to predict the response of the net CO_2 fluxes of arctic systems to climate change.

An earlier snowmelt, and a longer growing season does not necessarily translate into more carbon sequestered by high latitude ecosystems (Piao et al., 2020). There is large disagreement on the response of plant productivity and of the net CO_2 uptake to early snowmelt in tundra ecosystems (Humphreys and Lafleur, 2011; Parmentier et al., 2011; Lund et al., 2012; Ueyama et al. 2013; López-Blanco et al 2020). A warmer and longer growing season might not result in more net CO_2 uptake if CO_2 loss from respiration increases (Parmentier et al., 2011), particularly later in the season, is more than the CO_2 sequestered by enhanced plant productivity in northern ecosystems (Piao et al., 2008; Parmentier et al., 2011). Moreover, snowmelt timing and the growing season length greatly affect hydrologic conditions of Arctic soils (Liljedahl et al., 2016), as well as plant productivity (Park et al., 2016). Longer non frozen periods earlier in the year (Parida & Buermann, 2014), and earlier vegetation greening can increase evapotranspiration (ET), resulting in lower summer soil moisture (Angert et al., 2005; Buermann et al., 2018; Lian et al., 2020). The complexity in the hydrology of tundra systems comes from the tight link between the water drainage and the presence and depth of permafrost. The presence of permafrost reduces vertical water losses, preventing soil drainage in these northern wetlands during most of the summer despite low precipitation input (Rouse, 2000). Increasing rainfall (Zhang et al., 2013) and increased permafrost degradation can increase soil wetness in continuous permafrost regions (Liljedahl et al., 2016). Further permafrost degradation (e.g. ice-wedge melting) increases hydrologic connectivity leading to increased lateral drainage of the landscape and subsequent soil drying (Liljedahl et al., 2016, Christensen et al., 2020).

Given the importance of soil moisture in affecting the carbon balance of arctic ecosystems, and its links with snowmelt timing, in this study we investigated the correlation between summer fluxes of CO_2 (i.e., net ecosystem exchange (NEE), gross primary productivity (GPP) ecosystem respiration (ER)), ET, and environmental drivers such as soil moisture, vapor pressure deficit (VPD) and snowmelt timing, while controlling for the other most important drivers of photosynthesis and respiration (such as solar radiation, and air temperature). We expected earlier snowmelt to be correlated with larger ET, lower soil moisture, and a higher VPD particularly during peak and late season, consistent with drying associated with a longer growing season. The lower soil moisture with earlier snowmelt should result in a negative correlation between snowmelt timing and GPP particularly during the peak and late season (when we expect the most water stress), and in a positive correlation between snowmelt timing and ER during the entire growing season. This soil moisture limitation to plant productivity should result in lower net cumulative CO_2 sequestration during the entire summer (because of lower plant productivity if these ecosystems are water limited due to lower soil moisture with earlier snowmelt). Given that northern ecosystems are considered to be mostly temperature limited, we also tested if warmer conditions were associated with higher productivity and net CO_2 sequestration. We expect that higher temperatures were associated with higher GPP, and ER, but not with higher net CO_2 sequestration if ER increases more than GPP.

Testing the impact of snowmelt timing on the carbon dynamics and hydrology of tundra ecosystems. The 11 sites were selected as among the longest running tower sites in the circumpolar Arctic (including 6 to 19 years of fluxes per site, Table S1). All sites lie in zones of continuous permafrost regions, including a total of 119 site-years (summer only: June to August) of eddy covariance CO_2 flux data. These sites are representative of dominant tundra vegetation (wetland, graminoids, and shrub tundra), together accounting for 31% of all tundra vegetation types (Fig. 1, Walker et al., 2005 and Supplementary Information). Given the complex interactions among different variables (many covarying together), we used a variety of statistical analyses to identify the association between the standardized anomalies of NEE, GPP, ER, and ET, and the standardized anomalies of main environmental controls during different times of the summer corresponding to various stages in seasonal phenology (early season: June, peak season: July, and late season: August). A partial correlation analysis was used to identify if the timing of the snowmelt associates with anomalies of ET, soil moisture, NEE, GPP, ER, VPD, or the Bowen ratio (the ratio between Sensible Heat (H) and Latent Heat (LE)) while considering key meteorological forcing such as air temperature and solar radiation (Methods). Identifying the correlation between ET (and the Bowen ratio) and snowmelt timing is a way to assess water limitation to ecosystems (in addition to testing their response of soil moisture changes), as H and therefore the Bowen ratio are expected to increase with surface drying (Stiegler et al., 2016; Vourlitis and Oechel, 1997). To identify the association between the snowmelt timing, the main environmental variables (i.e., air temperature and solar radiation), and NEE, GPP, ER and ET over time, we performed a maximum covariance analysis (MCA) on the monthly median standardized anomalies from 2004-2019 (a time period when most of the sites had data available) retaining sites as the unit of variation. MCA allowed us to find patterns in two space-time datasets that are highly correlated using a cross-covariance matrix (Lian et al., 2020). The goal of this analysis was to identify the most important environmental drivers associated with NEE, GPP, and ER across all the sites over time. MCA is appropriate for this study as it can handle data with gaps and unequal lengths in the datasets. Finally, to evaluate the water balance at different times of the season, we estimated the difference between

Potential Evapotranspiration (PET) and the actual ET, and the difference between precipitation (PPT) and ET for each of the sites, years, and months (e.g. June, July, and August). This study did not attempt to describe the long-term temporal changes in the anomalies of snowmelt and carbon fluxes, given the short data record available for some of the sites (i.e. less than 10 years, Table S1), but focused on understanding the association between environmental variables and the carbon balance at different times of the season. More details of these analyses are included in the Methods.

Influence of snowmelt timing on NEE, GPP, ER, and hydrological status of tundra ecosystems. Once taking the variability in solar radiation and air temperature into account (in a partial correlation, Methods), we observed a significant positive relationship between the snowmelt timing anomalies and NEE anomalies (i.e. earlier snowmelt was associated with a higher net CO_2 sequestration) in June and July, but a negative correlation in August (Fig. 2a, Table 1). A similar relationship was found between snowmelt date anomalies and GPP anomalies, with more positive GPP anomalies (i.e. higher plant productivity) with earlier snowmelt in June and July, and more negative GPP anomalies with earlier snowmelt in August (Fig. 2b, Table 1). Earlier snowmelt was associated with significantly higher ER in both June and July, but there was no significant relationship in August (Fig. 2c, Table 1), suggesting that the late season correlation between NEE and snowmelt timing was mostly driven by the negative correlation between GPP and snowmelt in August. The MCA analysis showed that the anomalies in snowmelt timing had the highest squared covariance fraction (SCF) with the monthly median anomalies of GPP, NEE, and ER in June and July, and the lowest in

August over the 2004-2019 period (Fig. 3, Fig. S3-5). In late season, other environmental variables had a higher covariance with the GPP, NEE, and ER anomalies than the snowmelt timing, with VPD showing the highest SCF (Fig. 3, Fig. S3-5).

This result is consistent with the discrepancy between the observed increase in the maxNDVI over the last four decades, and the time integrated (TI) NDVI which instead has plateaued in the last two decades and even decreased over the last 10 years in several northern arctic ecosystems (Bhatt et al., 2021). TI-NDVI considers the length of the growing season and phenological variations (Tucker and Sellers 1986), and therefore better integrates the vegetation development during the entire growing season. Moisture has been shown to be important for the NDVI trends (Bhatt et al., 2021; Arndt et al., 2019). Given the potential water limitation to summer carbon uptake in northern ecosystems (Gonsamo et al., 2019; Agert et al., 2005; Parida & Buermann, 2014; Buermann et al., 2018), we tested if an earlier snowmelt was associated with a decrease in soil moisture which would affect GPP and NEE. We only observed a significant (and positive) correlation between soil moisture anomalies and snowmelt date anomalies in June (i.e. higher soil moisture with earlier snowmelt, Fig. S1a, Table S2), but no significant correlation in July and August (Fig. S1a, Table S2). The higher soil moisture with earlier snowmelt is consistent with surface inundation after snowmelt (Bowling et al., 2003; Woo et al., 2006) and earlier soil thawing resulting in higher soil moisture (i.e., soil moisture is low while soils are frozen). A similar result was observed for the ET anomalies: the higher ET with earlier snowmelt in June (Fig. S1b) could be the result of surface inundation after snowmelt (Vourlitis and Oechel, 1997). The standardized NEE anomalies were significantly correlated with the soil moisture anomalies in each of the summer months (Fig. S1d, Table S2). However the relationship between the GPP (and ER anomalies) and soil moisture anomalies was only significant in June (Fig. S1e,f, Table S2) suggesting soil moisture did not affect plant productivity (and respiration) in peak and late season, and the early season positive association might have been mostly driven by an earlier activation of the vegetation with earlier soil thaw (and the associated higher soil moisture). A higher water loss from ET in early season (Fig. S1b) could have resulted in the drying of the surface moss layer with the progression of the summer, which would have been consistent with the observed lower GPP and the lower net CO_2 sequestration with earlier snowmelt observed in August (Fig. 2a,b, Table 1). A potential moisture limitation to plant productivity might have been consistent also with the highest SCF of GPP and VPD anomalies in August than in June and July (Fig. S3). However, no significant relationship between ET (or soil moisture) and snowmelt date anomalies was observed in July and August (Fig. S1a,b) contrary to what would be expected if drying occurred following earlier snowmelt. No significant relationship was found between VPD anomalies and snowmelt date anomalies in any of the summer months (P=0.14 in a partial correlation considering air temperature and solar radiation anomalies). Finally, surface drying should result in an increase in the Bowen ratio anomalies with the progression of the summer, given that H increases with a decrease in water table and surface drying (Vourlitis and Oechel, 1997; Goeckede et al., 2017). However, the Bowen ratio showed no correlation with the standardized snowmelt date anomalies in any of the summer months (Fig. S1c, Table S2), and presented similar values in all the summer months (Fig. S2a). Anomalies in GPP and ER anomalies were positively correlated with both air temperature anomalies in all the summer months with no significant difference among the months (Fig. 2e,f). These results suggest that temperature (and not moisture) might still be the main limitation to plant growth in these arctic systems. The lack of correlation between the Bowen ratio and snowmelt date anomalies suggests that an earlier snowmelt did not result in significant surface drying. The median PET-ET, the median PPT-ET for all the years and sites included in this analysis (Fig.S2b,c) was also similar in June and July, and slightly higher in August, as reported by others for Russian arctic tundra (Runkle et al. 2014 and Goeckede et al. 2017). Although these analyses do not consider runoff, which can be significant (Liliendahl, et al., 2017; Lian et al., 2020), overall our results do not suggest that an earlier snowmelt resulted in a water stress (possibly from runoff anomalies) that significantly limited plant productivity in these continuous permafrost ecosystems.

The negative correlation between the anomalies in the August GPP and snowmelt timing is consistent with earlier senescence in northern plant species (e.g. *Eriophorum vaginatum*, a dominant species across these tundra types) compared to southern species growing in the same location in a common garden experiment (Parker et al., 2017). The phenotypic variation was shown to be persisting for decades (Souther et al., 2014), and ecotypes may be unable to extend the length of their growing season and might not be able to take advantage of a longer growing season (Parker et al., 2017). Several studies showed that once plant growth is initiated after the snowmelt in northern ecosystems, it continues only for a fixed number of days until the occurrence of senescence across several plant functional types (Bjorkman et al., 2015; Rosa et al., 2015; Semenchuk et al., 2016). Therefore, the lower GPP in August with earlier snowmelt might not be linked to water limitation to photosynthesis later in the season, but to an earlier senescence arising from endogenous rhythm of growth and senescence that plant functional types living in these extreme conditions developed over decades. An earlier senescence with an earlier start of the growing season after snowmelt in northern ecosystems is consistent with the earlier spring zero- crossing date and an earlier autumn zero-crossing date of the mean detrended seasonal CO_2 variations at Barrow, AK , USA (NOAA ESRL: https://www.esrl.noaa.gov/gmd/ccgg/obspack/) (Piao et al., 2020) during 2013–2017 than during 1980–1984. The spring and autumn zero-crossing date is the time when the detrended seasonal CO_2 variations intersect the zero line in spring and autumn respectively, and can be used as indicator for the start and end of the net CO_2 uptake by vegetation (Keeling et al., 1996; Piao et al., 2017). On the other hand, NDVI measurements show both an earlier start of the season, and a later end of season from 1982-1986 to 2008-2012 (Piao et al., 2020). The disagreement between the detrended seasonal atmospheric CO_2 concentration showing an earlier autumn zero-crossing date, and the NDVI measurements showing a later end of season has been explained by the increase in respiration in the fall (Piao et al., 2008). Similar to studies showing a higher increase in ER than in GPP with warming (Piao et al., 2008: Parmentier et al., 2011) we found that higher temperature, while increasing both GPP and ER, resulted in more net CO_2 sequestration only in June (Fig. 2d). The disagreement between atmospheric CO_2 concentration (showing an earlier autumn zero-crossing date), and NDVI (showing a later end of season, Piao et al., 2020) may also be explained by the challenges in using NDVI as a proxy for plant productivity in these arctic systems. NDVI has been shown to have a very variable and non-linear relationship with CO_2 fluxes and plant productivity (Beamish et al., 2020). While some arctic ecosystems showed that NDVI was strongly correlated with GPP (explaining 75% of the variation in GPP, Street et al., 2007), other studies showed that NDVI was either not significantly correlated with GPP and NEE (Zona et al., 2010) or was only able to explain a minor fraction (maximum of 25%) of the variation in NEE and GPP in some of these arctic tundra ecosystems (once accounting for the seasonal variation, La Puma et al., 2007; Olivas et al., 2011).

In conclusion, earlier snowmelt was associated with more net CO_2 uptake and higher GPP in early and peak season, but less net CO_2 uptake and lower GPP later in the summer, in arctic tundra ecosystems. We could not find evidence of a water limitation to GPP in the late season. We also found that warmer air temperatures were associated with higher plant productivity and ecosystem respiration, but only with higher net CO_2 sequestration in June. Although several hypotheses can be forwarded to explain the link between snowmelt and late-season declines in carbon uptake and in plant productivity, the current literature does not provide a definitive explanation (schematic Fig. 4). Future studies should investigate the potential interaction of different processes explaining the response of the carbon dynamics in the Arctic to warming and an earlier snowmelt, and reconstruct the temporal changes in the carbon balance from these systems. The link between the long-term changes in the CO_2 fluxes and NDVI should be better assessed in tundra ecosystems. It should be identified if higher NDVI is associated with higher net CO_2 uptake. In fact, greening of the Arctic might not necessarily translate into more net CO_2 uptake, as early and peak season carbon gains might be offset by a late season CO_2 loss, and respiration might counterbalance the increase in plant productivity. A better understanding of the processes driving these temporal changes is a fundamental step in advancing our prediction of the response of the arctic CO_2 balance to changing climate.

Materials and Methods

Site description

A total of 11 eddy covariance flux tower sites across the Arctic were used in this study, where each site had at least six summers of flux data available (SI, Table S1). Ecosystem-scale CO_2 fluxes were estimated using the eddy covariance method (Burba et al., 2008, Burba et al., 2012, Burba et al., 2013). Details pertaining to the sites, data processing, and gap-filling are provided in the SI Appendix, Table S1. All sites are located in continuous permafrost tundra regions. The vegetation in the tower sites, the instruments used to measure fluxes, the average environmental conditions at each site, the datasets used in this study for each site, and the references describing the sites are indicated in SI Appendix, Table S1. As shown in Fig. S2, the Bowen ratio reported for this study showed similar values to what previously reported during the growing season months in the Arctic (from 3.9 in a dry heath to 1.6 in a wet fen in Greenland, Stiegler et al., 2016; 0.83 Goeckede et al., 2017 to 0.20-0.25 in two Siberian Arctic sites, Runkle et al., 2014; and 0.51-1.69 in a moist-tussock tundra in Alaska, Vourlitis and Oechel, 1994).

To estimate the standardized anomalies in the soil moisture we selected the most consistent depths and sensors (the same sensor available for the entire time period in each site, or sensors at the most similar depths in each site and across sites when data from the same sensor was not available due to instrument failure). The number of sensors and the soil depths in each of the sites used for all the analyses were: (CA-DL1: N=2, one in a wet location and one in a dry location (both at -10 cm depth); US-Atq: N=1 (2010-2019) (-10 cm depth); US-Ivo: N=4 at -5 cm depth; US-Bes: N= 2 (2 diagonally inserted at 0-

10cm); US-Che: N=2 (-8cm and -16cm depth); RU-Sam: N=5 (at -5, -14, in rims at -5, -12, -15 cm depths in the center of ice-wedge polygons); US-ICt: N=2 (at -2.5 cm depth); GL-ZaH: N=2 (2000-2004 vertical 0-6 cm and from 2005 onward are at two horizontal depths : -5cm, -10 cm); CA-TVC: included one sensor inserted horizontally at -20cm depth. More details on the temporal coverage of the soil moisture data from each site are included in the Supplementary Table S1.

The R package 'Evapotranspiration' (Version 1.15, Guo et al., 2016) was used to estimate the daily aggregated Priestley-Taylor potential evaporation (McMahon et al., 2012; Priestley and Taylor, 1972) in each of the study sites, then summed into a monthly total and subtracted by the monthly total actual ET measured with eddy covariance in the respective sites to estimate the PET-ET shown in Fig. S2b. Raster files of monthly precipitation accumulation were acquired for the months of June-August from TerraClimate (Abaatzoglou et al., 2018) over the years 1959-2019. Precipitation data was then extracted from the Eddy Covariance tower coordinates using the terra package (Hijmans 2021) in R (R Core Development Team, 2020) to estimate a monthly total precipitation for June, July, and August for each of the sites included in this study (Tables S1). We did not use the precipitation collected by the meteorological sensors installed in the tower sites given the gaps in the site-level dataset. The other environmental variables used in this study were collected at the towers' sites. The median difference between the total precipitation and the total ET in each site was estimated to evaluate the PPT-ET in each study site during each time of the season (June, July, and August as shown in Fig. S2c). The median was used as it is less affected by outliers.

Statistical analysis

Site-level data

For the analyses performed in this study we separated the data into different times of the season (early season: June, peak season: July, late season: August), given that some of the environmental controls could be very different given the distinct stages of vegetation development. A partial correlation analysis was carried out to identify the correlation between the monthly median standardized anomalies (the ratio between the anomalies and the climatological standard deviation) of NEE, GPP, ER, ET, snow melt date and other environmental variables (most of which covary). The NEE, GPP, ER data used in these analyses were gap-filled using standard methodologies as described in the Supplementary Information. The partial correlations tested the relationships between the standardized snowmelt date anomalies and the monthly median standardized anomalies of NEE, GPP, ER, ET, VPD, and soil moisture, retaining sites as the unit of variation (while controlling for solar radiation and air temperature anomalies, main controls on carbon fluxes). The monthly scale was chosen as a more appropriate temporal scale to identify the importance of the variability in soil moisture on CO_2 fluxes (given that soil moisture does not change much at the hourly and weekly scale at these tundra sites). We also tested if the inclusion of site within a linear mixed model changed the results of correlation analysis between the anomalies. To this purpose, linear mixed effects models (nlme package in R, version R4.0.5, R Developing Team) were used to test the significance of the correlation between the above-mentioned anomalies, by including "site" as categorical random effects to account for pseudo-replication due to the different sites measured in different years. Model performance was evaluated based on the Akaike information criterion (AIC) values, on the marginal coefficient of determination (R^2_m similar to the explanatory power of the linear models) for generalized mixed-effects models as output by the "r.squaredGLMM" function within the "MuMIn" package in R (Nakagawa et al., 2013; Johnson et al., 2014). Given the very similar results between the partial correlation and the linear mixed modelling, we only included the results of the partial correlation and linear regression analyses in Table 1, and Table S2.

To maximize the dataset for each analysis we included all available time periods for the variables regressed in Fig. 2, but only selected the 2004-2019 period for the Maximum Covariance Analysis (MCA) analysis to include a time period where most sites had data available. The MCA was performed on two fields (e.g. anomalies in NEE and anomalies in snowmelt timing, see Fig. 3, Figs. S3-5); the columns of the two fields are spatial locations (each site was retained as a unit of variation of this analysis) and rows are temporal measurements. The first pair of singular vectors are the phase-space directions when projected that have the largest possible cross-covariance. The singular vectors describe the patterns in the anomalies that are linearly correlated. We used the time series of the first singular value decomposition (SVD) mode to visualize the parts of the datasets that vary together and report the squared covariance fraction (SCF) with the MCA (Fig. 3, Fig. S3-5). Given the limited length of the dataset we did not discuss the long-term changes in the reported anomalies. However, the MCA allowed us to evaluate the influence of snowmelt timing on the carbon balance over time at different times of the growing season. All analyses were carried out in R version 4.0.5 (R Core Team 2021).

Data Availability

The eddy covariance data from RU-Che, RU-Cok, and GL-ZaH (previously named DK-ZaH), CA-DL1, were obtained from the European Fluxes Database (http://www.europe-fluxdata.eu/home), from the Ameriflux Database (http://ameriflux.lbl.gov/), with some updated versions provided directly by the principal investigators of each site (e.g. the data from GL-ZaH are also available on: https://data.g-e-m.dk). The data from US-ICh and US-ICs are stored in the http://aon.iab.uaf.edu/data_access. US-Bes, US-Atq, US-Ivo are stored in the Arctic Data Center (Donatella Zona. 2019. Greenhouse gas flux measurements at the zero curtain, North Slope, Alaska, 2012-2019. Arctic Data Center. doi:10.18739/A2X34MS1B).

Tables

Table 1 Significance (P) and Pearson's correlation coefficient (r) of the relationships between the indicated monthly median standardized anomalies for June, July, and August retaining site as unit of variation. The anomalies of the indicated variables were regressed with air temperature anomalies in a simple linear regression, and with snow depth anomalies using a partial correlation accounting for the anomalies of solar radiation and air temperature, as shown in Fig. 2. The slopes of the regression between air temperature anomalies and GPP and ER anomalies were not significantly different between the different months but we reported the correlations tested for each month separately. The r value was only included when the P<0.1 (given that for P>0.1 we assumed that r is not different from zero).

Regression model	**month**	**P**	**r**
NEE ~ snow melt | Rg & air T	June	<0.001	0.42
	July	0.040	0.21
	August	<0.001	-0.48
GPP ~ snow melt | Rg & air T	June	<0.001	-0.52
	July	0.001	-0.33
	August	0.0074	0.27
ER ~ snow melt | Rg & air T	June	<0.001	-0.38
	July	<0.001	-0.34
	August	0.67	-
NEE ~ air T	June	<0.001	-0.35
	July	0.63	-
	August	0.45	-
GPP ~ air T	June	<0.001	0.47
	July	0.0092	0.27
	August	0.0021	0.31
ER ~ air T	June	<0.001	0.45
	July	<0.001	0.39
	August	<0.001	0.40

Figures and figure legends

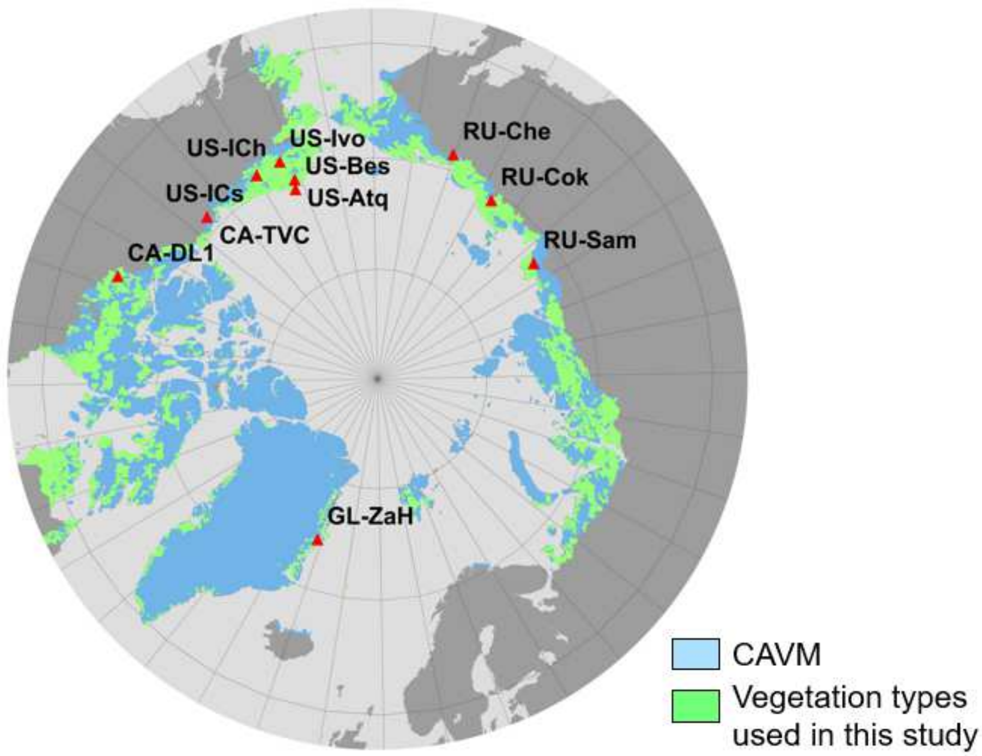

Figure 1 | Study sites. The 11 eddy covariance flux tower sites used in this study. Light blue regions delineate the total Circumpolar Arctic Vegetation Map (CAVM). Green regions delineate the subset of CAVM vegetation types used in this study (including all the vegetation types listed in Table S1).

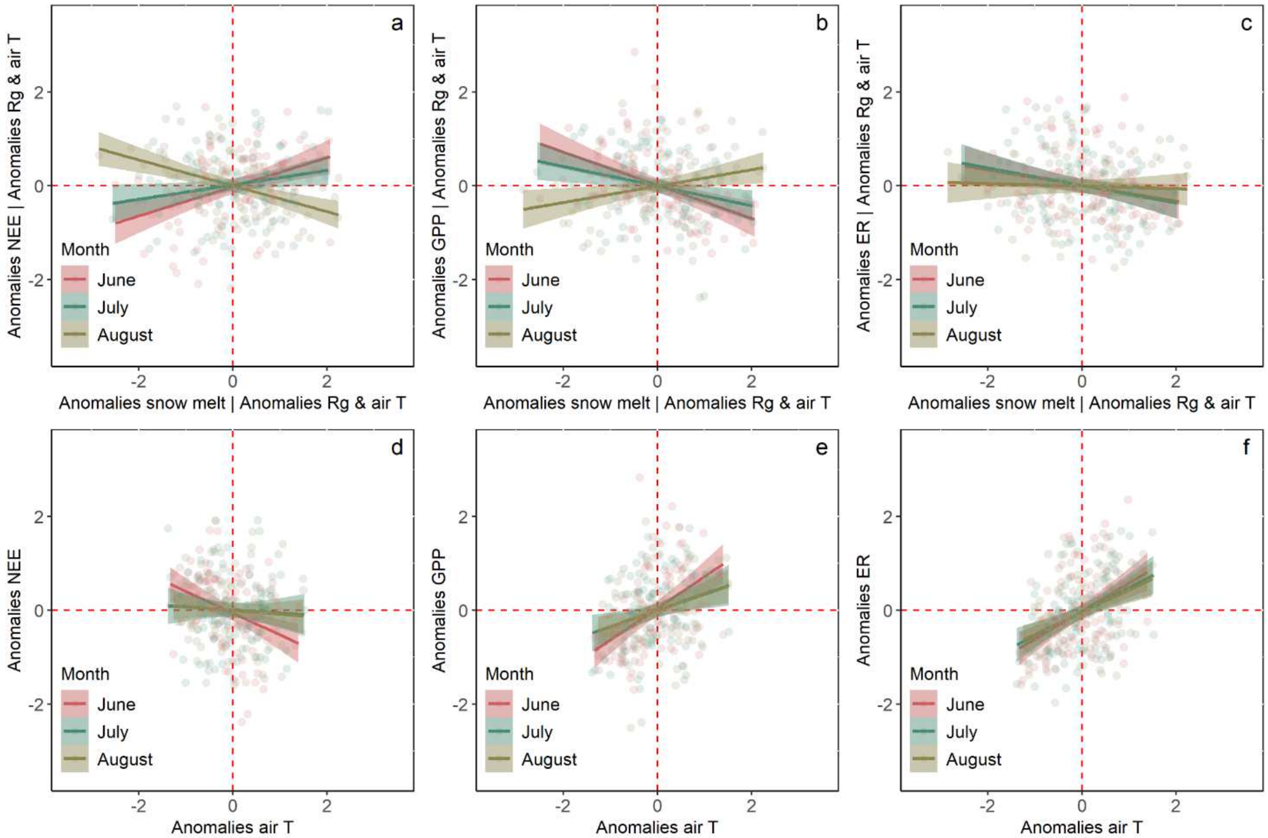

Figure 2 | Relationships between the indicated median monthly anomalies using linear regressions and partial correlation accounting for solar radiation and air temperature anomalies (retaining site as the unit of variation). Given that the interaction term between "month" and snowmelt timing was significant, we included the correlation coefficients and P of the regressions for each of the indicated months in Table 1 (shaded areas are 95% Confidence Intervals). Negative values indicate CO_2 uptake and positive values CO_2 release into the atmosphere.

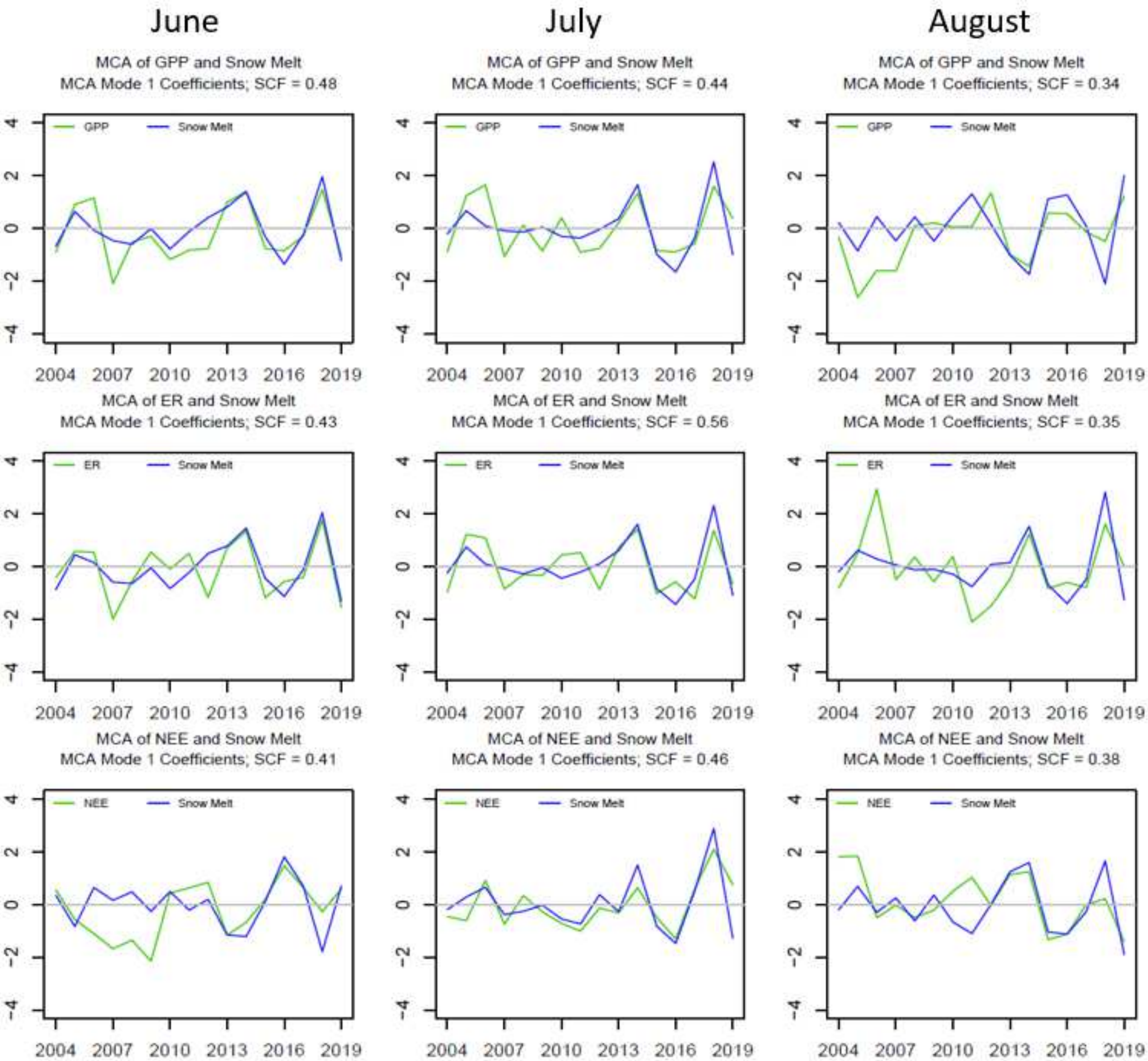

Figure 3 | Maximum covariance analysis (MCA) for the June, July, and August monthly median of the indicated anomalies. The first pair of singular vectors are the phase-space directions when projected that have the largest possible cross-covariance. The singular vectors describe the patterns in the anomalies that are linearly correlated. Displayed is the time series of the first singular value decomposition (SVD) mode which visualizes the parts of the datasets that vary together and included above each panel is the squared covariance fraction (SCF) of each couple of variables. A similar trend and a higher SCF indicates a stronger association over time between the indicated variables.

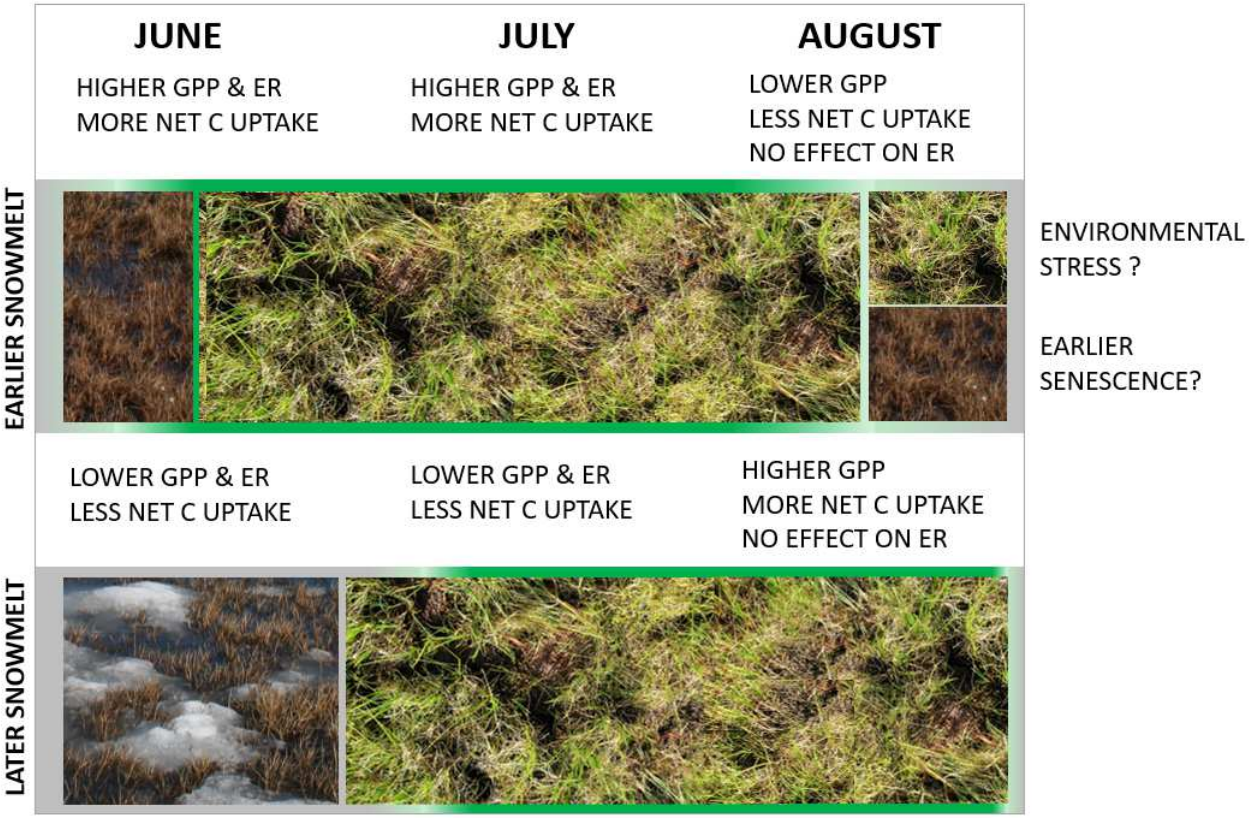

Figure 4 | Schematic of the effect of earlier snowmelt on NEE, GPP, and ER at different times of the season. Earlier snowmelt results in an earlier activation of the vegetation and higher plant productivity and higher net carbon uptake in June and July. This earlier activation could result in a more carbon loss and lower productivity with earlier snowmelt in August, potentially related to either environmental stress or for an earlier senescence.

Acknowledgements

The complete list of funding bodies that supported this study is included in the SI Appendix. DZ, WCO, XX, and DAL acknowledge support from the Office of Polar Programs of the National Science Foundation (NSF) (award number 1204263, and 1702797) with additional logistical support funded by the NSF Office of Polar Programs, from the NASA Carbon in Arctic Reservoirs Vulnerability Experiment (CARVE), an Earth Ventures (EV-1) investigation, under contract with the National Aeronautics and Space Administration, and from the NASA ABoVE (NNX15AT74A; NNX16AF94A) Program. The Alaskan sites are located on land owned by the Ukpeagvik Inupiat Corporation (UIC). This project has received funding from the European Union's Horizon 2020 research and innovation program under grant agreement No. 727890, and by the Natural Environment Research Council (NERC) UAMS Grant (NE/P002552/1), and from the NOAA Cooperative Science Center for Earth System Sciences and Remote Sensing Technologies (NOAA-CESSRST) under the Cooperative Agreement Grant # NA16SEC4810008. Additional support was provided by NOAA Cooperative Science Center for Earth System Sciences and Remote Sensing Technologies (NOAA-CESSRST) under the Cooperative Agreement Grant NA16SEC4810008. Part of the analysis was carried out in part at the Jet Propulsion Laboratory, California Institute of Technology, under a contract with the National Aeronautics and Space Administration (80NM0018D0004).

References

Abatzoglou JT, Dobrowski SZ, Parks SA, Hegewisch KC. TerraClimate, a high-resolution global dataset of monthly climate and climatic water balance from 1958–2015. Scientific Data 5, 170191 (2018).

Angert A, et al. Drier summers cancel out the CO2 uptake enhancement induced by warmer springs. Proceedings of the National Academy of Sciences of the United States of America 102, 10823-10827 (2005).

Arndt KA, et al. Arctic greening associated with lengthening growing seasons in Northern Alaska. Environmental Research Letters 14, 125018 (2019).

Beamish A, et al. Recent trends and remaining challenges for optical remote sensing of Arctic tundra vegetation: A review and outlook. Remote Sensing of Environment 246, 111872 (2020).

Berner, L. T. et al. Summer warming explains widespread but not uniform greening in the Arctic tundra biome. Nature Communications 11, 4621, doi:10.1038/s41467-020-18479-5 (2020).

Bhatt US, et al. Climate drivers of Arctic tundra variability and change using an indicators framework. Environmental Research Letters 16, 055019 (2021).

Boike J, et al. (2019) A 16-year record (2002–2017) of permafrost, active-layer, and meteorological conditions at the Samoylov Island Arctic permafrost research site, Lena River delta, northern Siberia: an opportunity to validate remote-sensing data and land surface, snow, and permafrost models. Earth Syst. Sci. Data 11(1):261-299.

Bowling LC, Kane DL, Gieck RE, Hinzman LD, Lettenmaier DP. The role of surface storage in a low-gradient Arctic watershed. Water Resources Research 39, (2003).

Bruhwiler, L., Parmentier, F.-J. W., Crill, P., Leonard, M. & Palmer, P. I. The Arctic Carbon Cycle and Its Response to Changing Climate. Current Climate Change Reports 7, 14-34, doi:10.1007/s40641-020-00169-5 (2021).

Buermann W, et al. Widespread seasonal compensation effects of spring warming on northern plant productivity. Nature 562, 110-114 (2018).

Burba G Eddy Covariance Method for Scientific, Industrial, Agricultural and Regulatory Applications: a Field Book on Measuring Ecosystem Gas Exchange and Areal Emission Rates. LI-COR Biosciences, Lincoln, USA, 331 pp. ISBN: 978-0-61576827-4(2013).

Burba G, et al. Calculating CO2 and H2O eddy covariance fluxes from an enclosed gas analyzer using an instantaneous mixing ratio. Glob Change Biol 18(1), 385-399 (2012).

Burba GG, McDermitt DK, Grelle A, Anderson DJ, & Xu L Addressing the influence of instrument surface heat exchange on the measurements of CO2 flux from open-path gas analyzers. Glob Change Biol 14(8):1854-1876 (2008).

Christensen TR, et al. Multiple Ecosystem Effects of Extreme Weather Events in the Arctic. Ecosystems 24, 122-136 (2021).

Euskirchen ES, Bret-Harte MS, Shaver GR, Edgar CW, & Romanovsky VE (2017) Long-Term Release of Carbon Dioxide from Arctic Tundra Ecosystems in Alaska. Ecosystems 20(5):960-974.

Euskirchen ES, et al. (2006) Importance of recent shifts in soil thermal dynamics on growing season length, productivity, and carbon sequestration in terrestrial high-latitude ecosystems. Glob Change Biol 12(4):731-750.

Forbes, B. C., Fauria, M. M. & Zetterberg, P. Russian Arctic warming and 'greening' are closely tracked by tundra shrub willows. Glob. Change Biol. 16, 1542-1554, doi:10.1111/j.1365-2486.2009.02047.x (2010).

Gamm, C. M. et al. Declining growth of deciduous shrubs in the warming climate of continental western Greenland. Journal of Ecology 106, 640-654, doi:https://doi.org/10.1111/1365-2745.12882 (2018).

Goeckede, M, et al. Shifted energy fluxes, increased Bowen ratios, and reduced thaw depths linked with drainage-induced changes in permafrost ecosystem structure. The Cryosphere 11, 2975-2996 (2017).

Gonsamo, A., Ter-Mikaelian, M. T., Chen, J. M. & Chen, J. Does Earlier and Increased Spring Plant Growth Lead to Reduced Summer Soil Moisture and Plant Growth on Landscapes Typical of Tundra-Taiga Interface? Remote Sensing 11, 1989 (2019).

Goodrich JP, et al. (2016) Impact of different eddy covariance sensors, site set-up, and maintenance on the annual balance of CO2 and CH4 in the harsh Arctic environment. Agr Forest Meteorol 228-229:239-251.

Guo D, Westra S, Maier HR. An R package for modelling actual, potential and reference evapotranspiration. Environmental Modelling & Software 78, 216-224 (2016).

Helbig, M. et al. Addressing a systematic bias in carbon dioxide flux measurements with the EC150 and the IRGASON open-path gas analyzers. Agricultural and Forest Meteorology 228-229, 349-359, doi:https://doi.org/10.1016/j.agrformet.2016.07.018 (2016).

Hijmans RJ terra: Spatial Data Analysis. R package version 1.1-4. https://CRAN.R-project.org/package=terra (2021).

Holl D, et al. (2019) A long-term (2002 to 2017) record of closed-path and open-path eddy covariance CO2 net ecosystem exchange fluxes from the Siberian Arctic. Earth Syst. Sci. Data 11(1):221-240.

Humphreys ER & Lafleur PM (2011) Does earlier snowmelt lead to greater CO2 sequestration in two low Arctic tundra ecosystems? Geophys Res Lett 38(9), doi:10.1029/2011GL047339.

Johnson PCD. Extension of Nakagawa & Schielzeth's R2GLMM to random slopes models. Methods in Ecology and Evolution 5, 944-946 (2014).

Kade A, Bret-Harte MS, Euskirchen ES, Edgar C, & Fulweber RA (2012) Upscaling of CO2 fluxes from heterogeneous tundra plant communities in Arctic Alaska. J Geophys Res-Biogeo 117(G4).

Keeling CD, Chin JFS, Whorf TP. Increased activity of northern vegetation inferred from atmospheric CO2 measurements. Nature 382, 146-149 (1996).

Kwon, M. J. et al. Drainage enhances modern soil carbon contribution but reduces old soil carbon contribution to ecosystem respiration in tundra ecosystems. Glob. Change Biol. 25, 1315-1325, doi:10.1111/gcb.14578 (2019).

La Puma IP, Philippi TE, Oberbauer SF. Relating NDVI to ecosystem CO2 exchange patterns in response to season length and soil warming manipulations in arctic Alaska. Remote Sensing of Environment 109, 225-236 (2007). https://doi.org/10.1016/j.rse.2007.01.001.

Lafleur PM & Humphreys ER (2008) Spring warming and carbon dioxide exchange over low Arctic tundra in central Canada. Glob Change Biol 14: 740–756.

Lara, M. J., Nitze, I., Grosse, G., Martin, P. & McGuire, A. D. Reduced arctic tundra productivity linked with landform and climate change interactions. Sci. Rep. 8, 2345 (2018).

Lian X, et al. Summer soil drying exacerbated by earlier spring greening of northern vegetation. Science Advances 6, eaax0255 (2020).

Liljedahl AK, et al. Pan-Arctic ice-wedge degradation in warming permafrost and its influence on tundra hydrology. Nature Geosci 9:312, doi:10.1038/ngeo2674. (2016).

Liljedahl AK, Hinzman LD, Kane DL, Oechel WC, Tweedie CE, Zona DE. Tundra water budget and implications of precipitation underestimation. Water Resour Res 53, 6472-6486 (2017).

López-Blanco E, et al. Multi-year data-model evaluation reveals the importance of nutrient availability over climate in arctic ecosystem C dynamics. Environmental Research Letters 15, 094007 (2020).

Lucht, W. et al. Climatic control of the high- latitude vegetation greening trend and Pinatubo effect. Science. 296, 1687–1689 (2002).

Lund M, et al. (2012) Trends in CO2 exchange in a high Arctic tundra heath, 2000–2010. J Geophys Res-Biogeo 117(G2), doi:10.1029/2011jg001901.

McMahon TA, Peel MC, Lowe L, Srikanthan R, McVicar TR. Estimating actual, potential, reference crop and pan evaporation using standard meteorological data: a pragmatic synthesis. Hydrol Earth Syst Sci 17, 1331-1363 (2013).

Miles, V. V. & Esau, I. Spatial heterogeneity of greening and browning between and within bioclimatic zones in northern West Siberia. Environ. Res. Lett. 11, 115002 (2016).

Mudryk L., R. Brown, C. Derksen, K. Luojus, B. Decharme, and S. Helfrich (2019) Terrestrial snow cover, Richter-Menge, J., M. L. Druckenmiller, and M. Jeffries, Eds.: Arctic Report Card 2019, https://www.arctic.noaa.gov/Report-Card.

Mudryk LR, Kushner PJ, Derksen C, Thackeray C. Snow cover response to temperature in observational and climate model ensembles. Geophys Res Lett. 2017;44:919–26. https://doi.org/10.1002/2016GL071789.

Myers-Smith, I. H. et al. Complexity revealed in the greening of the Arctic. Nature Climate Change 10, 106-117, doi:10.1038/s41558-019-0688-1 (2020).

Nakagawa S, Schielzeth H. A general and simple method for obtaining R2 from generalized linear mixed-effects models. Methods in Ecology and Evolution 4, 133-142 (2013).

Oechel WC, Laskowski CA, Burba G, Gioli B, & Kalhori AAM (2014) Annual patterns and budget of CO2 flux in an Arctic tussock tundra ecosystem. J Geophys Res-Biogeo 119(3):323-339, doi:10.1002/2013JG002431.

Olivas PC, Oberbauer SF, Tweedie C, Oechel WC, Lin D, Kuchy A. Effects of Fine-Scale Topography on CO2 Flux Components of Alaskan Coastal Plain Tundra: Response to Contrasting Growing Seasons. Arctic, Antarctic, and Alpine Research 43, 256-266 (2011).

Overland JE, Hanna E, Hanssen-Bauer I, Kim S-J, Walsh JE, Wang M, et al. In: The NOAA Arctic Report Card, Surface Air Temperature 2019, https://arctic.noaa.gov/Report-Card/Report-Card 2019/ArtMID/7916/ArticleID/835/Surface-Air-Temperature.

Papale, D. & Valentini, R. A new assessment of European forests carbon exchanges by eddy fluxes and artificial neural network spatialization. Glob. Change Biol. 9, 525-535, doi:10.1046/j.1365-2486.2003.00609.x (2003).

Parida BR, Buermann W. Increasing summer drying in North American ecosystems in response to longer nonfrozen periods. Geophysical Research Letters 41, 5476-5483

(2014).

Park T, et al. Changes in growing season duration and productivity of northern vegetation inferred from long-term remote sensing data. Environmental Research Letters 11, 084001 (2016).

Parker TC, Tang J, Clark MB, Moody MM, Fetcher N. Ecotypic differences in the phenology of the tundra species Eriophorum vaginatum reflect sites of origin. Ecol Evol 7, 9775-9786 (2017).

Parmentier FJW, et al. Spatial and temporal dynamics in eddy covariance observations of methane fluxes at a tundra site in northeastern Siberia. Journal of Geophysical Research: Biogeosciences 116, G03016 (2011).

Piao S, et al. Characteristics, drivers and feedbacks of global greening. Nature Reviews Earth & Environment 1, 14-27 (2020).

Piao S, et al. Net carbon dioxide losses of northern ecosystems in response to autumn warming. Nature 451, 49-52 (2008).

Piao S, et al. Weakening temperature control on the interannual variations of spring carbon uptake across northern lands. Nature Climate Change 7, 359-363 (2017).

Priestley, C & Taylor, R. On the assessment of surface heat flux and evaporation using largescale parameters. Monthly Weather Review, vol. 100, no. 2, pp. 81-92 (1972).

R Core Development Team. (2020). R: A language and environment for statistical computing v. 4.0.2. Vienna: R Foundation for Statistical Computing.

R Core Team (2019). R: A language and environment for statistical computing. R Foundation for Statistical Computing, Vienna, Austria. URL https://www.R-project.org/.

Rosa RK, et al. Plant phenological responses to a long-term experimental extension of growing season and soil warming in the tussock tundra of Alaska. Glob Chang Biol 21, 4520-4532 (2015).

Rouse, W. R.: The energy and water balance of high-latitude wetlands: controls and extrapolation, Glob. Change Biol., 6, 59–68, 2000.

Runkle BRK, Wille C, Gažovič M, Wilmking M, Kutzbach L. The surface energy balance and its drivers in a boreal peatland fen of northwestern Russia. Journal of Hydrology 511, 359-373 (2014).

Sachs, T., Giebels, M. , Boike, J. and Kutzbach, L. (2010), Environmental controls on CH4 emission from polygonal tundra on the microsite scale in the Lena river delta, Siberia. Global Change Biology, 16: 3096-3110. doi:10.1111/j.1365-2486.2010.02232.x

Semenchuk PR, Gillespie MAK, Rumpf SB, Baggesen N, Elberling B, Cooper EJ. High

Arctic plant phenology is determined by snowmelt patterns but duration of phenological periods is fixed: an example of periodicity. Environmental Research Letters 11, 125006 (2016).

Souther, S, Fetcher, N, Fowler, Z, Shaver, GR, & McGraw, JB Ecotypic differentiation in photosynthesis and growth of Eriophorum vaginatum along a latitudinal gradient in the Arctic tundra. Botany 92, 551-561 (2014).

Stiegler, C., Lund, M., Christensen, T. R., Mastepanov, M., and Lindroth, A.: Two years with extreme and little snowfall: effects on energy partitioning and surface energy exchange in a high-Arctic tundra ecosystem, The Cryosphere, 10, 1395–1413, https://doi.org/10.5194/tc-10-1395-2016, 2016.

Street LE, Shaver GR, Williams M, Van Wijk MT. What is the relationship between changes in canopy leaf area and changes in photosynthetic CO2 flux in arctic ecosystems? Journal of Ecology 95, 139-150 (2007).

Tucker CJ, Sellers PJ. Satellite remote sensing of primary production. International Journal of Remote Sensing 7, 1395-1416 (1986).

Ueyama M, et al. (2013) Growing season and spatial variations of carbon fluxes of Arctic and boreal ecosystems in Alaska (USA). Ecol Appl 23(8):1798-1816, doi:10.1890/11-0875.1.

Vourlitis GL, Oechel WC. Landscape-Scale CO2 H2O Vapour and Energy Flux of Moist-Wet Coastal Tundra Ecosystems over Two Growing Seasons. Journal of Ecology 85, 575-590 (1997).

Walker DA, et al. Phytomass, LAI, and NDVI in northern Alaska: Relationships to summer warmth, soil pH, plant functional types, and extrapolation to the circumpolar Arctic. J Geophys Res-Atmos 108(D2) (2003).

Walker DA, et al. The Circumpolar Arctic vegetation map. Journal of Vegetation Science 16(3):267-282, doi:10.1111/j.1654-1103.2005.tb02365.x (2005).

Walker DA, Gould WA, Maier HA, & Raynolds MK The Circumpolar Arctic Vegetation Map: AVHRR-derived base maps, environmental controls, and integrated mapping procedures. Int J Remote Sens 23(21):4551-4570 (2002).

Woo M-k, Young KL, Brown L. High Arctic Patchy Wetlands: Hydrologic Variability and Their Sustainability. Physical Geography 27, 297-307 (2006).

Zhang X, et al. On the variation of regional CO2 exchange over temperate and boreal North America. Global Biogeochemical Cycles 27, 2012GB004383 (2013).

Zona D, et al. Cold season emissions dominate the Arctic tundra methane budget. Proc Natl Acad Sci USA 113(1):40-45 (2016).

Zona D, Oechel WC, Peterson KM, Clements RJ, Paw U KT, Ustin SL. Characterization of the carbon fluxes of a vegetated drained lake basin chronosequence on the Alaskan Arctic Coastal Plain. Glob Change Biol 16, 1870-1882 (2010).

Supplementary Files

This is a list of supplementary files associated with this preprint. Click to download.

- Supplementaryinformation20211006.pdf